

LETTER

Open Access

Fluid-metapelite interaction in an ultramafic mélange: implications for mass transfer along the slab-mantle interface in subduction zones

Yasushi Mori^{1*}, Miki Shigeno¹ and Tadao Nishiyama²

Abstract

The slab-mantle interface in subduction zones is a site of tectonic mixing of crustal and mantle rocks. It is the interface for fluid flow of slab-derived components into the mantle wedge. To assess the fluid-rock interaction along the slab-mantle interface, we studied the bleaching of pelitic schist in an ultramafic mélange. The Nishisonogi metamorphic rocks in Kyushu, Japan, comprise ultramafic mélanges intercalated with epidote-blueschist facies schists. The ultramafic mélange consists of tectonic blocks of various lithologies and a matrix of chlorite-actinolite schist and serpentinite. Along the contact with the mélange matrix, pelitic schist blocks are bleached mainly due to the modal increase of albite and the consumption of carbonaceous material. The bleaching is probably attributed to infiltration of Na-rich external fluid from the mélange matrix. Mass balance analysis indicates losses of C, Rb, K₂O, Ba, Pb, and SiO₂ from the bleached pelitic schist, although Al₂O₃, TiO₂, Sc, Y, Zr, Nb, La, Ce, and Nd remain immobile. This suggests fractionation of large-ion lithophile elements (LILE) and Pb from the high-field-strength elements and rare earth elements during the bleaching. If this ultramafic mélange is analogous to the slab-mantle interface, similar infiltration metasomatism will promote liberation of C, Si, LILE, and Pb from subducting metapelites and enhance metasomatism of the mantle wedge.

Keywords: Element fractionation; Fluid-rock interaction; Metapelite; Subduction zone mélange; Nishisonogi metamorphic rocks

Findings

Introduction

Fluid flow is an agent of large-scale mass transfer in subduction zones and plays a key role in mantle metasomatism and arc magmatism (Peacock 1990; Bebout 1996, 2007a, 2007b, 2013; Manning 2004; Klemd 2013; Spandler and Pirard 2013). At great depths in subduction zones (15 to 100 km), fluids (aqueous fluids in shallower levels and possibly silicate melts in deeper levels; *cf.* Bebout 2007a, b) derived from subducting slabs can transport various components into the mantle wedge, causing hydration and metasomatism of the mantle (Maury et al. 1992; Ryan et al. 1996; Morris and Ryan 2003; Schmidt and Poli 2003; Rüpke et al. 2004). It is generally believed that such fluid flow is essential to generate arc magmas with elevated

concentrations of fluid-mobile components such as large-ion lithophile elements (LILE; e.g., Ba, K, Rb, Cs), B, U, and Pb (Morris et al. 1990; Hawkesworth et al. 1993; Tatsumi and Eggins 1995; Davidson 1996; Elliott 2003).

Recent studies of subduction zone mélanges have revealed that significant fluid flow and fluid-rock interaction took place along the slab-mantle interface (Bebout and Barton 1989, 1993, 2002; Sorensen and Grossman 1989, 1993; King et al. 2003, 2006, 2007; Breeding et al. 2004; Marschall et al. 2006; Spandler et al. 2008; Miller et al. 2009; Penniston-Dorland et al. 2010, 2012). The mélanges represent tectonic and metasomatic mixing of sedimentary, mafic, and ultramafic rocks along the interface region at the contact between the subducting slab and the mantle wedge. The mixing may involve devolatilization reactions that would not occur during simple (essentially closed-system) metamorphism of each lithology. Moreover, fluid-rock interactions or exchanges between the sedimentary and ultramafic rocks will produce new hybrid rocks. The

* Correspondence: mori@kmnh.jp

¹Kitakyushu Museum of Natural History and Human History, 2-4-1 Higashida, Yahatahigashi-ku, Kitakyushu 805-0071, Japan

Full list of author information is available at the end of the article

hybrid rocks have the potential to take up and release components distinct from the protoliths. Thus, fluid-rock interaction in mélanges probably affects the mass transfer of slab-derived components into the wedge mantle.

This paper describes an example of fluid-metapelite interaction in a subduction zone mélange intercalated with epidote-blueschist facies schists. Metapelites are the most important reservoirs of LILE in subducting slabs. Mass balance analysis provides evidence of the liberation of C, Si, LILE, and Pb from metapelites during infiltration metasomatism.

Geological background

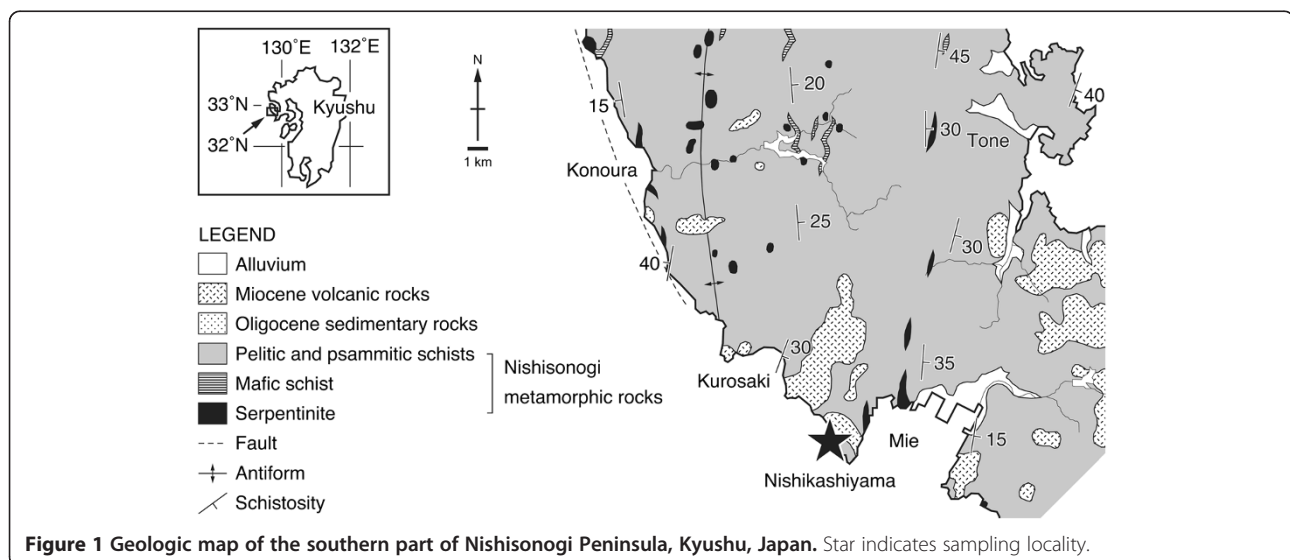
The Nishisonogi metamorphic rocks in Kyushu, Japan, represent a Late Cretaceous subduction complex that consists of epidote-blueschist facies schists with minor serpentinite (Figure 1). The schists include mainly pelitic, psammitic, and mafic lithologies. Phengitic muscovite in the pelitic and psammitic schists yields K-Ar and $^{40}\text{Ar}/^{39}\text{Ar}$ plateau ages of 85 to 60 Ma (Hattori and Shibata 1982; Faure et al. 1988). The matrix mineral assemblages of the pelitic and psammitic schists are carbonaceous material + garnet + chlorite + muscovite + albite + quartz \pm epidote and albite + muscovite + quartz \pm chlorite, respectively. The psammitic schist locally contains glaucophane + epidote/piemontite + hematite + rutile \pm garnet in the matrix. The mafic schist occurs as conformable layers (<100 m in thickness) within the pelitic and psammitic schists. The matrix mineral assemblages of the mafic schist are actinolite/barroisite + epidote + chlorite + albite \pm quartz and glaucophane + epidote + chlorite + albite + hematite \pm quartz, with the former assemblage being dominant. The serpentinite, which is in tectonic contact with the schists, occurs as pod-like bodies (<150 m in diameter) and ultramafic mélanges

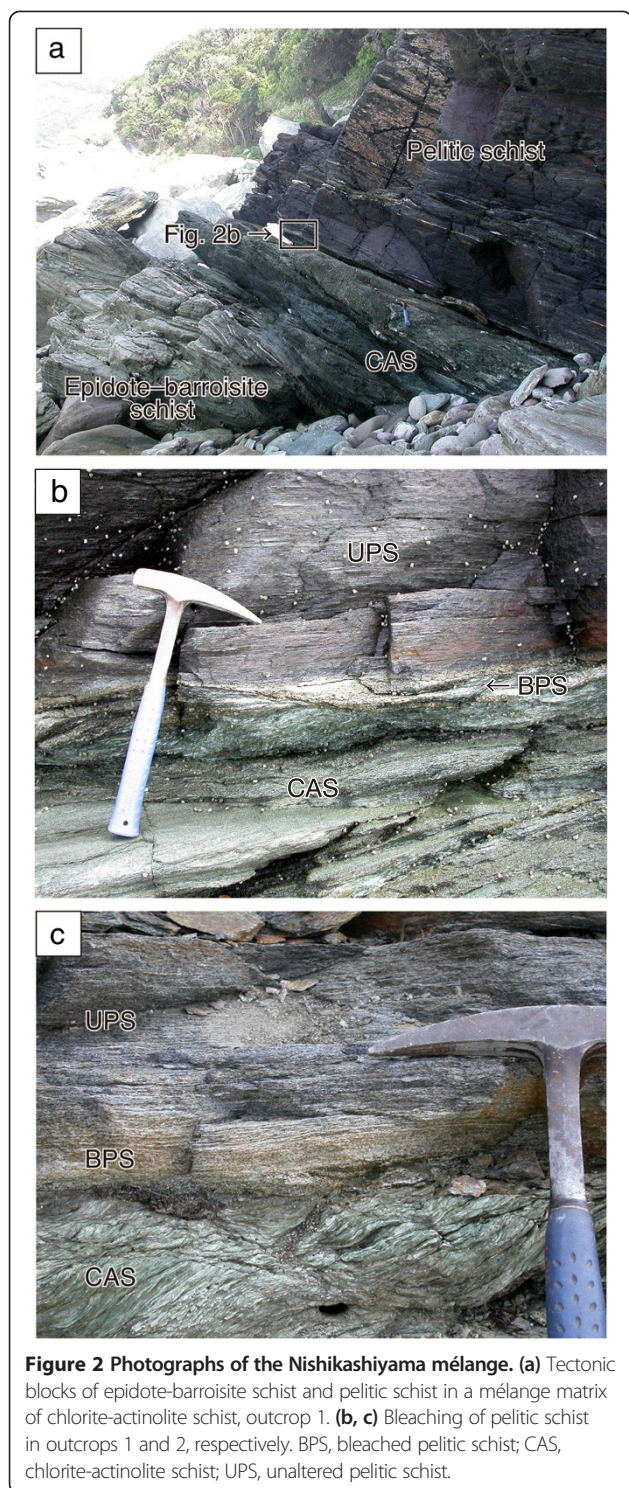
(<350 m in thickness). The serpentinite pods typically have metasomatic rinds (Uchida and Muta 1957, 1958; Mori et al. 2007). The matrix mineral assemblage of the serpentinite is antigorite + magnetite \pm dolomite \pm magnesite \pm talc; chrysotile and lizardite are rare. The ultramafic mélanges contain tectonic blocks of metagabbro, mafic schist, pelitic schist, and albitite in a matrix of chlorite-actinolite schist, talc schist, and schistose serpentinite (Nishiyama 1989, 1990). Small blocks (<5 m in diameter) of jadeitite, omphacite, rodingite, and zoisite are found locally (Nishiyama 1978; Shigeno et al. 2005, 2012a, b; Mori et al. 2011).

One of the largest ultramafic mélanges in the study area is exposed at Nishikashiyama district in Nagasaki, Japan (Figure 1). A wide variety of rocks such as epidote-barroisite schist, epidote-glaucophane schist, pelitic schist, and albitite appear as discrete tabular blocks less than 10 m in thickness (Figure 2a). These blocks are mutually isolated by a mélange matrix (<5 m in thickness) of chlorite-actinolite schist. The mélange matrix locally contains thin lenses (<2 m in thickness) of serpentinite. In this mélange, all pelitic schist blocks show bleaching along the contact with the mélange matrix (Figure 2b,c). The pelitic schist is normally black but becomes white when within several centimeters of the mélange matrix. The boundary between the unaltered part and bleached part of the pelitic schist is parallel to the contact.

Sampling and analytical methods

To study the bleaching of pelitic schist blocks, samples were collected from two outcrops in Nishikashiyama (Figure 2b, c). From each outcrop, one sample of bleached pelitic schist (BPS), three samples of neighboring unaltered pelitic schist (UPS), and one sample of chlorite-actinolite schist (CAS) were taken. The BPS and UPS





represent different stratigraphic layers of pelitic schist; sampling along a single layer was not possible.

The minerals in the samples were examined with a polarizing microscope under transmitted and reflected light. The modal compositions were measured by counting 2,000 points with a grid interval of 0.1 mm for each

sample. Fluid inclusions and opaque minerals were analyzed with a Horiba Jobin Yvon LabRAM HR800 Raman spectrometer (HORIBA Jobin Yvon Inc., Edison, NJ, USA) equipped with a 514-nm argon ion laser housed at Kumamoto University, Japan.

The whole-rock compositions of the samples were determined with a PANalytical MagiX Pro X-ray fluorescence (XRF) spectrometer (PANalytical B.V., Almelo, The Netherlands) and a PerkinElmer 2400 II CHN element analyzer (PerkinElmer, Waltham, MA, USA) housed at the Kitakyushu Museum of Natural History and Human History, Japan. About 300 g of each sample was powdered and homogenized. About 4 g of the sample powder was heated to 950°C for 3 h to measure loss on ignition (LOI). Then, 1 g of the heated powder was prepared as a 1:5 dilution glass bead for XRF. The details of the XRF analysis followed the method of Mori and Mashima (2005). About 0.2 g of the unheated powder was used for CHN (H₂O and C) analysis. Finally, the XRF, LOI, and CHN data were combined as whole-rock compositions.

Petrography

Photomicrographs of the samples are shown in Figure 3. Modal compositions are shown in Figure 4.

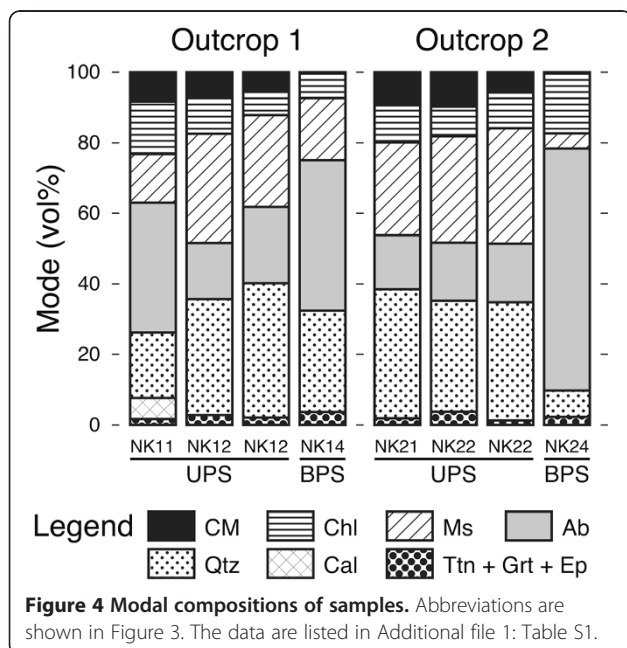
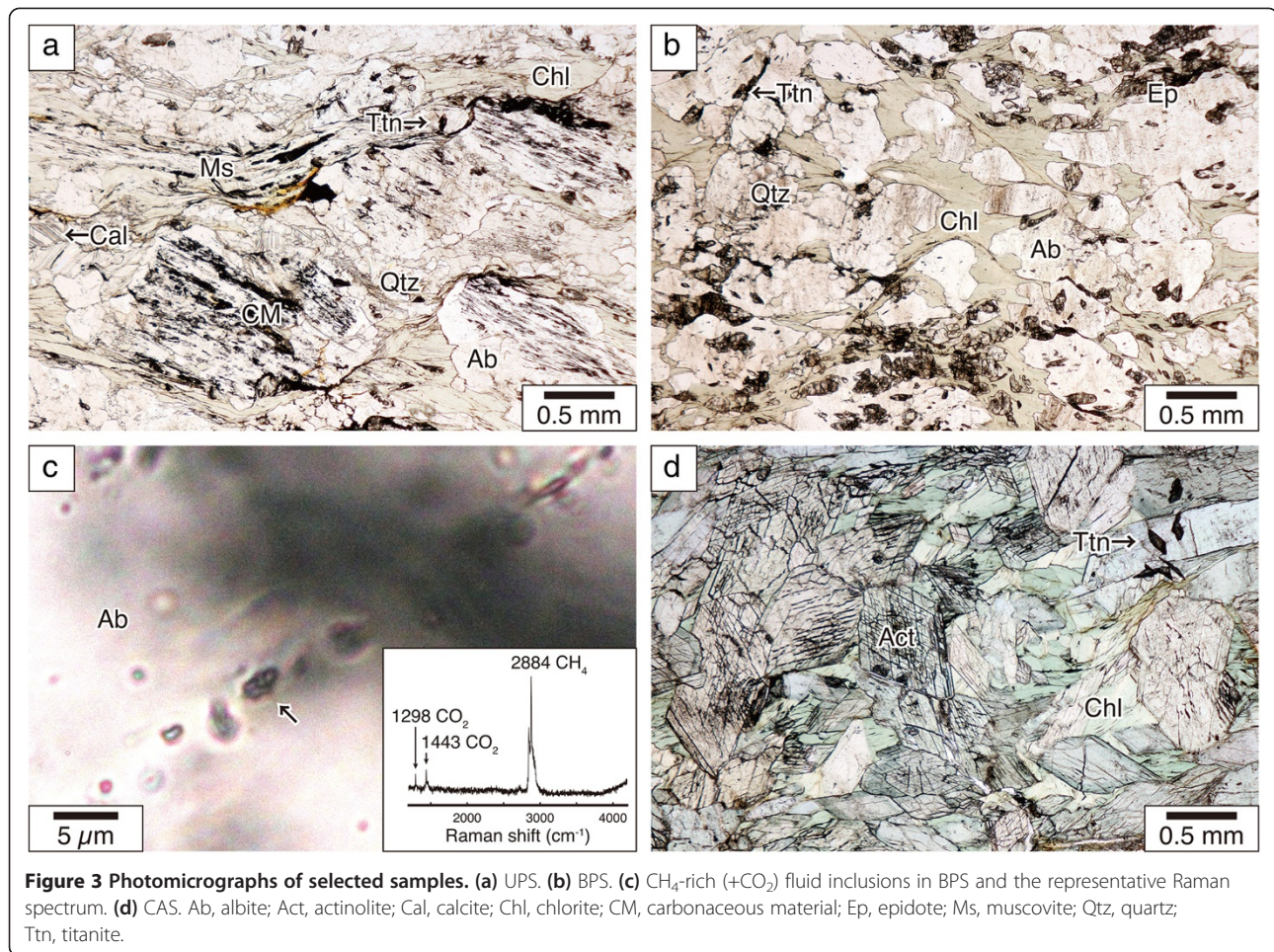
Unaltered pelitic schist

The mineral assemblage of UPS is carbonaceous material + chlorite + muscovite + albite + quartz + titanite ± garnet ± calcite ± epidote (Figure 3a). Ore minerals are rare. A minor amount of accessory tourmaline is present in some samples. Carbonaceous material is 5 to 9 vol% in the mode and occurs either as a matrix mineral or as inclusions in albite. It contains graphite and disordered carbons and is considered metamorphosed organic matter. Albite (15 to 37 vol%) typically occurs as porphyroblasts of 1 to 2 mm in diameter. Chlorite (7 to 15 vol%) and muscovite (14 to 33 vol%) define the schistosity of the UPS. Quartz is 19 to 38 vol% in the mode. Titanite is present in all the UPS samples.

Bleached pelitic schist

The mineral assemblage of the BPS is chlorite + muscovite + albite + quartz + titanite ± epidote (Figure 3b). This is essentially the same as the mineral assemblage of the UPS except for the notable absence of carbonaceous material. The BPS lacks carbonaceous material not only in the matrix but also in the albite porphyroblasts. The modal compositions indicate that the BPS is richer in albite (43 and 69 vol% in outcrops 1 and 2, respectively) and is generally poorer in muscovite (18 and 4 vol%) and quartz (29 and 8 vol%) than the UPS. Titanite is present in all the BPS samples.

The albite porphyroblasts have numerous fluid inclusions along clusters of healed microcracks (Figure 3c). This



is a feature not found in UPS. The fluid inclusions are typically less than 5 μm in size, have round shapes, and are filled by one phase (H₂O liquid) or two phases (liquid and a small gas bubble) at room temperature. There are two types of the two-phase inclusions: CH₄-rich (±CO₂) inclusions and H₂O inclusions. There is no obvious difference in the mode of occurrence of these two types.

Chlorite-actinolite schist

The mineral assemblage of the CAS is actinolite + chlorite + titanite + albite ± tourmaline (Figure 3d). The actinolite is dominant in the mode (85 and 93 vol% in outcrops 1 and 2, respectively), defines the schistosity, and occurs as euhedral grains of 0.1 to 5 cm long. Chlorite, titanite, and albite occur in the interstices among the actinolite grains.

Whole-rock chemistry

The whole-rock compositions of the samples are listed in Additional file 1: Table S1. As shown in Figure 4, carbonaceous material is the major reservoir of carbon. The sample NK11 contains both carbonaceous material and calcite (Figure 4), but division between C and CO₂ is

difficult. Thus, carbon in all the samples is regarded as C in the mass balance analysis discussed below.

Discussion

Bleaching process of pelitic schist

The bleaching of the pelitic schist involves the changes in mineralogy and whole-rock chemistry. There are two possible mechanisms. As the UPS is a boundary layer, it may represent diffusive exchange of components between the pelitic schist and ultramafic mélangé matrix. Boundary flow of external fluids may cause infiltration metasomatism of the pelitic schist.

To examine the bleaching mechanisms, the chemical mass balance between the UPS and BPS was estimated using the isocon method (Grant 1986). As shown in Figure 2, the UPS gradually changes into the BPS upon approaching the margin of the pelitic schist block. There are no structural discontinuities between them, in contrast to the contact between the BPS and CAS. Thus, the UPS is considered the protolith of the BPS. In each outcrop, the average composition of the UPS was used as the unaltered reference frame. We regarded the standard deviation of the UPS compositions as the inherent heterogeneity of the protolith and used it to calculate the uncertainties of the mass balance analysis (Baumgartner and Olsen 1995).

The isocon diagrams for the BPS are shown in Figure 5. The isocon is defined by TiO_2 , Al_2O_3 , P_2O_5 , Sc, Y, Zr, Nb, La, Ce, and Nd. These components are thought to be immobile in this metasomatic system. In outcrop 1, the isocon slope ($=1.11 \pm 0.03$) indicates that the UPS had lost 10% of its bulk mass during the bleaching. The elemental mass changes include losses of 15% SiO_2 , 23% K_2O , 95% C, 47% Rb, 21% Ba, and 47% Pb, along with gains of 33% MgO, 34% Na_2O , 109% Ni, and 161% Cu, relative to the protolith values. The isocon diagram for outcrop 2 shows more dispersive distribution of data than that for outcrop 1, suggesting more intense metasomatism. In

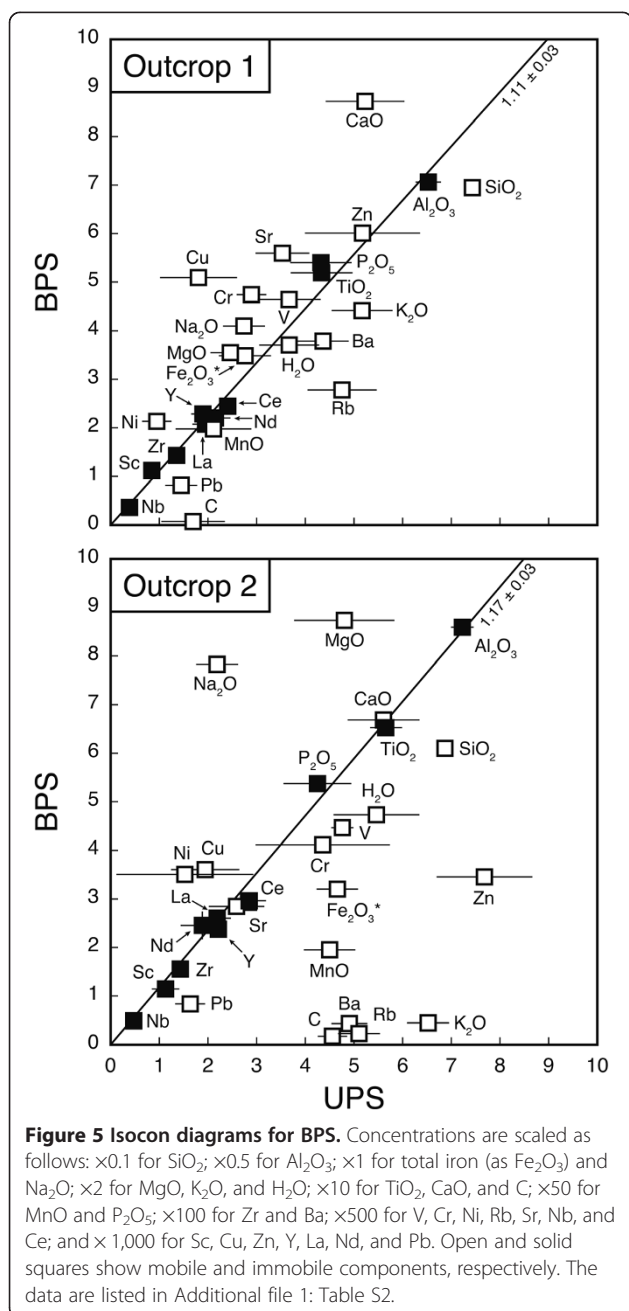


Table 1 Element mass changes in BPS

	Outcrop			
	1		2	
	Sample NK14	Sample NK24	Sample NK14	Sample NK24
	(g/100 g of protolith)	(% change)	(g/100 g of protolith)	(% change)
SiO_2	-11 ± 2	-15	-16 ± 2	-23
Fe_2O_3^a	$+0.4 \pm 0.5$	+14.9	-1.9 ± 0.4	-40.0
MnO	-0.00 ± 0.02	-11.87	-0.06 ± 0.01	-62.60
MgO	$+0.4 \pm 0.2$	+32.9	$+1.4 \pm 0.5$	+56.6
CaO	$+0.27 \pm 0.08$	+51.44	$+0.01 \pm 0.07$	+2.25
Na_2O	$+0.1 \pm 0.4$	+34.4	$+4.5 \pm 0.4$	+203.7
K_2O	-0.6 ± 0.3	-23.2	-3.1 ± 0.2	-93.4
H_2O	-0.16 ± 0.31	18.75	-0.7 ± 0.5	-25.1
C	-0.16 ± 0.07	-94.78	-0.44 ± 0.03	-95.70
	($\mu\text{g/g}$ of protolith)	(% change)	($\mu\text{g/g}$ of protolith)	(% change)
V	$+11 \pm 13$	+15	-19 ± 6	-19
Cr	$+28 \pm 6$	+48	-15 ± 28	-18
Ni	$+21 \pm 6$	+109	$+30 \pm 28$	+96
Cu	$+29 \pm 8$	+161	$+12 \pm 7$	+59
Zn	$+2 \pm 12$	+5	-47 ± 10	-61
Rb	-45 ± 14	-47	-98 ± 9	-95
Sr	$+32 \pm 11$	+46	-2 ± 12	-4
Ba	-92 ± 52	-21	-453 ± 36	-91
Pb	-7 ± 3	-7	-9 ± 3	-55

^aTotal iron as Fe_2O_3 .

outcrop 2, the isocon slope ($=1.17 \pm 0.03$) indicates that the UPS lost 14% of its bulk mass during the bleaching. The elemental mass changes include losses of 23% SiO_2 , 93% K_2O , 96% C, 95% Rb, 91% Ba, and 55% Pb, along with gains of 57% MgO, 204% Na_2O , 96% Ni, and 59% Cu, relative to the protolith values.

The chemical mass balance suggests that the bleaching of the pelitic schist is an open system with respect to some mobile components. For example, the significant gain of Na_2O (Table 1) is probably unable to explain by simple exchange between the pelitic schist and ultramafic mélangé matrix. As the Na_2O concentration is typically low in the ultramafic mélangé matrix, influx of Na-rich fluid would be necessary. Although the diffusive exchange of components is possible, the fluid flow and infiltration metasomatism are considered more important mechanisms of the bleaching.

Element mobility and mineral stability

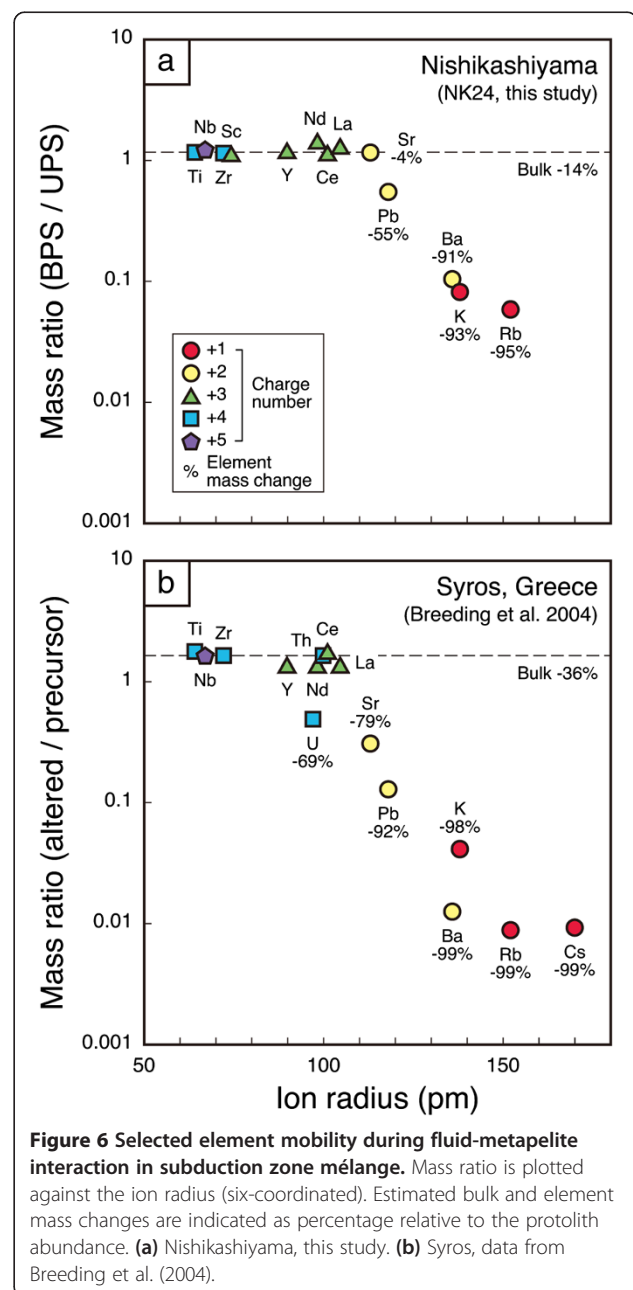
The elemental mass changes (Table 1) are coupled to the stability of the key host minerals in the BPS (Figure 4). The loss of SiO_2 and C corresponds to the decrease of quartz and the consumption of carbonaceous material, respectively. The loss of K_2O , Rb, and Ba is correlated with the decrease of muscovite. The gain of Na_2O and MgO reflects the increase of albite and chlorite, respectively. In outcrop 1, the gain of CaO and Sr is comparable with the increase of epidote [see Additional file 1: Table S1]. Some immobile components such as TiO_2 , Y, Nb, La, Ce, and Nd are probably held in titanite that remains stable. The mass change of total iron is inconsistent with the modal change. This may be because total iron contains ferric (mainly in epidote and chlorite) and ferrous oxides (mainly in chlorite).

A salient change during the bleaching of the pelitic schist is the consumption of carbonaceous material (Figures 3 and 4). As the BPS and CAS have the low C concentration and do not contain carbonate minerals, we infer that the infiltration of fluid from the mélangé matrix converted the carbonaceous material to carbonic fluids. If the infiltrating fluid is reducing relative to the pore fluid in the pelitic schist, the carbonaceous material will be converted to hydrocarbons (CH_4 , etc.). Alternatively, if the infiltrating fluid is oxidizing, the carbonaceous material will be converted to CO_2 . The CH_4 -rich ($\pm\text{CO}_2$) fluid inclusions in the BPS may be the traces of such processes (Figure 3c). Unfortunately, there are few records of the redox state of the fluids in the samples. Nishiyama (1990) described CO_2 metasomatism of an exposed metabasite block in the Mie mélangé 2.5 km northeast of Nishikashiyama (Figure 1). He speculated that the origin of the CO_2 -rich fluid ($X_{\text{CO}_2} > 0.785$) was the oxidation of carbonaceous material in pelitic schist blocks. However, such a process may not be a suitable explanation

for the case of the Nishikashiyama mélangé because the BPS and CAS contain titanite and actinolite (Figure 3b, d). These minerals are destabilized under high- X_{CO_2} conditions (cf. Nishiyama 1990).

Implications for mass transfer along the slab-mantle interface

The most striking result of the mass balance analysis is the obvious correlation between the elemental mass changes and the ion radius and charge number. As shown in Figure 6a, a significant mass of LILE (Rb, K, Ba) and Pb



with relatively large ion radii and low charge numbers is lost in the BPS. In contrast, the high-field-strength elements (HFSE; e.g., Ti, Nb, and Zr) and rare earth elements (REE; e.g., La, Ce, and Nd) remain immobile. Consequently, the infiltration metasomatism causes fractionation of LILE and Pb from the HFSE and REE along with the bleaching of the pelitic schist. Because the CAS has low concentrations of LILE and Pb [see Additional file 1: Table S2], these components are probably liberated from the pelitic schist blocks and migrate away via the fluid flow.

Breeding et al. (2004) reported similar fluid-metapelite interaction from an eclogite facies mélange exposed in Syros, Greece. Near the meta-ultramafic mélange matrix, the mineral assemblage of the metapelite was altered from phengite + sodic pyroxene + epidote + garnet + glaucophane + quartz + titanite + rutile + zircon to glaucophane + chlorite + albite + magnetite + apatite + titanite + rutile + zircon (Figure 6b). The difference between the mineralogical changes in Syros and Nishikashiyama probably reflects the difference in the *P-T* conditions of the fluid-metapelite interaction. Nevertheless, the elemental mass changes are similar (Figure 6). LILE, Pb, Sr, and U are significantly lost during the alteration, but the HFSE, REE, and Th remain nearly immobile. Such a fluid-metapelite interaction and element fractionation may occur at various depths (eclogite facies and epidote-blueschist facies to lower *P-T* conditions) along the slab-mantle interface in subduction zones.

Conclusions

This paper describes bleaching of pelitic schist blocks in an ultramafic mélange intercalated with epidote-blueschist facies schists of the Nishisonogi metamorphic rocks. The bleaching is attributed to infiltration of Na-rich external fluid and involves liberation of C (as carbonic fluids), Si, Rb, K, Ba, and Pb from the pelitic schist. Titanium, Nb, Zr, La, Ce, and Nd remain immobile, so the LILE and Pb are fractionated from the HFSE and REE. Such a fluid-metapelite interaction may occur at various depths along the slab-mantle interface that is the site of tectonic mixing of sedimentary, mafic, and ultramafic rocks. Therefore, ultramafic mélanges are a potential source of slab-derived components and play an important role in material recycling in subduction zones.

Additional file

Additional file 1: The file contains two tables showing modal compositions of samples (Table S1) and whole-rock compositions of samples (Table S2).

Abbreviations

Ab: albite; Act: actinolite; BPS: bleached pelitic schist; Cal: calcite; CAS: chlorite-actinolite schist; Chl: chlorite; CM: carbonaceous material; Ep: epidote; Ms: muscovite; Qtz: quartz; Ttn: titanite; UPS: unaltered pelitic schist.

Competing interests

The authors declare that they have no competing interests.

Authors' contributions

YM carried out the field investigation and sampling, performed the microscopic observation and analyses (Raman, XRF, CHN, and LOI), and drafted the manuscript. MS participated in the design of the study and helped in the field investigation, sampling, and CHN analysis. TN participated in the design of the study and helped in the field investigation and Raman analysis. All authors read and approved the final manuscript.

Authors' information

YM is a researcher/curator of petrology in Kitakyushu Museum of Natural History and Human History (KMNH). MS is a researcher of petrology/structural geology in KMNH. TN is a professor of petrology in Graduate School of Science and Technology, Kumamoto University.

Acknowledgements

This study is financially supported by Grant-in-Aid for Young Scientists B (Nos. 16740303 and 21740385 to YM) from Japan Society for the Promotion of Science and by Grant-in-Aid for Scientific Research A (No. 17204045 to TN) and Grant-in-Aid for Scientific Research C (No. 24540524 to YM) from the Ministry of Education, Culture, Sports, Science and Technology, Japan. We appreciate reviews and comments by T. Morishita and anonymous reviewers.

Author details

¹Kitakyushu Museum of Natural History and Human History, 2-4-1 Higashida, Yahatahigashi-ku, Kitakyushu 805-0071, Japan. ²Graduate School of Science and Technology, Kumamoto University, 2-39-1 Kurokami, Chuo-ku, Kumamoto 860-8555, Japan.

Received: 10 December 2013 Accepted: 16 April 2014

Published: 4 June 2014

References

- Baumgartner LP, Olsen SN (1995) A least-squares approach to mass transport calculations using the isocon method. *Econ Geol* 90:1261–1270
- Bebout GE (1996) Volatile transfer and recycling at convergent margins: mass-balance and insights from high-*P/T* metamorphic rocks. In: Bebout GE, Scholl DW, Kirby SH, Platt P (eds) Subduction top to bottom. American Geophysical Union, Geophysical Monograph series 96, Washington D.C, pp 179–193
- Bebout GE (2007a) Metamorphic chemical geodynamics of subduction zones. *Earth Planet Sci Lett* 260:373–393
- Bebout GE (2007b) Trace element and isotopic fluxes/subducted slab. *Treat Geochem* 3:1–50
- Bebout GE (2013) Metasomatism in subduction zones of subducted oceanic slabs, mantle wedges, and the slab-mantle interface. In: Harlov DE, Austrheim H (eds) Metasomatism and the chemical transformation of rocks. Lecture notes in earth system science, Springer, Berlin, pp 289–349
- Bebout GE, Barton MD (1989) Fluid flow and metasomatism in a subduction zone hydrothermal system: Catalina Schist terrane, California. *Geology* 17:976–980
- Bebout GE, Barton MD (1993) Metasomatism during subduction: products and possible paths in the Catalina Schist, California. *Chem Geol* 108:61–92
- Bebout GE, Barton MD (2002) Tectonic and metasomatic mixing in a high-*T*, subduction-zone mélange – insights into the geochemical evolution of the slab-mantle interface. *Chem Geol* 187:79–106
- Breeding CM, Ague JJ, Bröcker M (2004) Fluid-metasedimentary interactions in subduction zone mélange: implications for the chemical composition of arc magmas. *Geology* 32:1041–1044
- Davidson JP (1996) Deciphering mantle and crustal signature in subduction zone magmatism. In: Bebout GE, Scholl DW, Kirby SH, Platt P (eds) Subduction top to bottom. American Geophysical Union, Geophysical Monograph series 96, Washington D.C, pp 251–262
- Elliott T (2003) Tracers of the slab. In: Eiler J (ed) Inside the subduction factory. American Geophysical Union, Geophysical Monograph series 138, Washington D.C, pp 23–45
- Faure M, Fabbri O, Monie P (1988) The Miocene bending of southwest Japan: new ³⁹Ar/⁴⁰Ar and microtectonic constraints from the Nagasaki schists

- (western Kyushu), an extension of the Sanbagawa high-pressure belt. *Earth Planet Sci Lett* 91:105–116
- Grant JA (1986) The isocon diagram – a simple solution to Gresens' equation for metasomatic alteration. *Econ Geol* 81:1976–1982
- Hattori H, Shibata K (1982) Radiometric dating of pre-Neogene granitic and metamorphic rocks in northwest Kyushu, Japan – with emphasis on geotectonics of the Nishisonogi zone. *Bull Geol Surv Japan* 33:57–84
- Hawkesworth CJ, Gallagher K, Hergt JM, McDermott F (1993) Mantle and slab contributions in arc magmas. *Annu Rev Earth Planet Sci* 21:175–204
- King RL, Kohn MJ, Eiler JM (2003) Constraints on the petrologic structure of the subduction zone slab–mantle interface from Franciscan Complex exotic ultramafic blocks. *Geol Soc Am Bull* 115:1097–1109
- King RL, Bebout GE, Moriguchi T, Nakamura E (2006) Elemental mixing systematics and Sr-Nd isotope geochemistry of mélange formation: obstacles to identification of fluid sources to arc volcanism. *Earth Planet Sci Lett* 246:288–304
- King RL, Bebout GE, Grove M, Moriguchi T, Nakamura E (2007) Boron and lead isotope signatures of subduction-zone mélange formation: hybridization and fractionation along the slab–mantle interface beneath volcanic fronts. *Chem Geol* 239:305–322
- Klemm R (2013) Metasomatism during high-pressure metamorphism: eclogites and blueschist-facies rocks. In: Harlow DE, Austrheim H (eds) *Metasomatism and the chemical transformation of rocks*. Lecture notes in earth system science, Springer, Berlin, pp 351–413
- Manning CE (2004) The chemistry of subduction-zone fluids. *Earth Planet Sci Lett* 223:1–16
- Marschall HR, Ludwig T, Altherr R, Kalt A, Tonarini S (2006) Syros metasomatic tourmaline: evidence for very high- $\delta^{11}\text{B}$ fluids in subduction zones. *J Petrol* 47:1915–1942
- Maury RC, Defant MJ, Joron JL (1992) Metasomatism of the sub-arc mantle inferred from trace elements in Philippine xenoliths. *Nature* 360:661–663
- Miller DP, Marschall HR, Schumacher JC (2009) Metasomatic formation and petrology of blueschist-facies hybrid rocks from Syros (Greece): implications for reactions at the slab–mantle interface. *Lithos* 107:53–67
- Mori Y, Mashima H (2005) X-ray fluorescence analysis of major and trace elements in silicate rocks using 1:5 dilution glass beads. *Bull Kitakyushu Mus Nat Hist Hum Hist, Ser A* 3:1–12
- Mori Y, Nishiyama T, Yanagi T (2007) Chemical mass balance in a reaction zone between serpentinite and metapelites in the Nishisonogi metamorphic rocks, Kyushu, Japan: implications for devolatilization. *Island Arc* 16:28–39
- Mori Y, Orihashi Y, Miyamoto T, Shimada K, Shigeno M, Nishiyama T (2011) Origin of zircon in jadeitite from the Nishisonogi metamorphic rocks, Kyushu, Japan. *J Metamorphic Geol* 29:673–684
- Morris JD, Ryan JG (2003) Subduction zone processes and implications for changing composition of the upper and lower mantle. *Treat Geochem* 2:451–470
- Morris JD, Leeman WP, Tera F (1990) The subducted component in island arc lavas: constraints from Be isotopes B-Be systematics. *Nature* 344:31–36
- Nishiyama T (1978) Jadeitite from the Nishisonogi metamorphic region. *J Geol Soc Japan* 84:155–156 (in Japanese)
- Nishiyama T (1989) Petrologic study of the Nagasaki metamorphic rocks in the Nishisonogi peninsula – with special reference to the greenrock complex and the reaction-enhanced ductility. *Mem Geol Soc Japan* 33:237–257 (in Japanese with English abstract)
- Nishiyama T (1990) CO_2 -metasomatism of a metabasite block in a serpentinite melange from the Nishisonogi metamorphic rocks, southwest Japan. *Contrib Mineral Petrol* 104:35–46
- Peacock SM (1990) Fluid processes in subduction zones. *Science* 248:329–337
- Penniston-Dorland SC, Sorensen SS, Ash RD, Khadke SV (2010) Lithium isotopes as a tracer of fluids in a subduction zone mélange: Franciscan Complex, CA. *Earth Planet Sci Lett* 292:181–190
- Penniston-Dorland SC, Bebout GE, Pogge von Strandmann PAE, Elliott T (2012) Lithium and its isotopes as tracers of subduction zone fluids and metasomatic processes: evidence from the Catalina Schist, California, USA. *Geochim Cosmochim Acta* 77:530–545
- Rüpke LH, Morgan JP, Hort M, Connolly JAD (2004) Serpentinite and the subduction zone water cycle. *Earth Planet Sci Lett* 223:17–34
- Ryan J, Morris J, Bebout G, Leeman B (1996) Describing chemical fluxes in subduction zones: insights from “depth-profiling” studies of arc and forearc rocks. In: Bebout GE, Scholl DW, Kirby SH, Platt P (eds) *Subduction top to bottom*. American Geophysical Union, Geophysical Monograph series 96, Washington D.C., pp 263–268
- Schmidt MW, Poli S (2003) Generation of mobile components during subduction of oceanic crust. *Treat Geochem* 3:567–591
- Shigeno M, Mori Y, Nishiyama T (2005) Reaction microtextures in jadeitites from the Nishisonogi metamorphic rocks, Kyushu, Japan. *J Mineral Petrol Sci* 100:237–246
- Shigeno M, Mori Y, Shimada K, Nishiyama T (2012a) Origin of omphacites from the Nishisonogi metamorphic rocks, western Kyushu, Japan: comparison with jadeitites. *Eur J Mineral* 24:247–262
- Shigeno M, Mori Y, Shimada K, Nishiyama T (2012b) Jadeitites with metasomatic zoning from the Nishisonogi metamorphic rocks, western Japan: fluid–tectonic block interaction during exhumation. *Eur J Mineral* 24:289–311
- Sorensen SS, Grossman JN (1989) Enrichment of trace elements in garnet amphibolites from a paleo-subduction zone: Catalina Schist, southern California. *Geochim Cosmochim Acta* 53:3155–3177
- Sorensen SS, Grossman JN (1993) Accessory minerals and subduction zone metasomatism: a geochemical comparison of two mélanges (Washington and California, U.S.A.). *Chem Geol* 110:269–297
- Spandler C, Pirard C (2013) Element recycling from subducting slabs to arc crust: a review. *Lithos* 170–171:208–223
- Spandler C, Hermann J, Faure K, Mavrogenes JA, Arculus RJ (2008) The importance of talc and chlorite “hybrid” rocks for volatile recycling through subduction zones; evidence from the high-pressure subduction mélange of New Caledonia. *Contrib Mineral Petrol* 155:181–198
- Tatsumi Y, Eggins S (1995) *Subduction zone magmatism*. Blackwell Science, Oxford
- Uchida Y, Muta K (1957) The talc deposits in northern Kyushu (1) – the distribution and types of talc deposits –. *J Geol Soc Japan* 63:586–597 (in Japanese with English abstract)
- Uchida Y, Muta K (1958) The talc deposits in northern Kyushu (2) – on the talc deposits of the Nishisonogi type. *J Geol Soc Japan* 64:494–515 (in Japanese with English abstract)

doi:10.1186/1880-5981-66-47

Cite this article as: Mori et al.: Fluid-metapelite interaction in an ultramafic mélange: implications for mass transfer along the slab-mantle interface in subduction zones. *Earth, Planets and Space* 2014 **66**:47.

Submit your manuscript to a SpringerOpen[®] journal and benefit from:

- Convenient online submission
- Rigorous peer review
- Immediate publication on acceptance
- Open access: articles freely available online
- High visibility within the field
- Retaining the copyright to your article

Submit your next manuscript at ► springeropen.com